Original scientific paper
UDC: 662.756.3:620.91
DOI: 10.7251/afts.2016.0814.047M
COBISS.RS-ID 5845528

CERAMICS MATERIALS MICROSTRUCTURE PROGNOSIS WITHIN THE ALTERNATIVE ENERGY SOURCES AND STRUCTURE FRACTAL NATURE FRONTIERS

Mitić V. Vojislav[1,2], Kocić Ljubiša[1], Paunović Vesna[1], Bastić Filip[1,2]

[1]*University of Niš, Faculty of Electronic Engineering, Niš, Serbia, e-mail. vmitic.d2480@gmail.com*
[2]*Institute of Technical Sciences of SASA, Belgrade, Serbia e-mail.filip.bastic@gmail.com*

ABSTRACT

Doped ceramics materials structure can be controlled using different synergetic effects as well as consolidation parameters. Additives concentration influence on ceramics microstructure and dielectric properties, based on fractal geometry, is analyzed. These properties level control level is very important in advanced materials prognosis. The Coble's two-sphere model is used as initial one, for developing a new two-ellipsoid model; unlike the spherical geometry, the ellipsoidal-polyhedral geometry,besides better approximation of sintering particles, is in relation with consolidation parameters (sintering time and temperature). The experiments have been based on $BaTiO_3$ with different additives (CeO_2, $MnCO_3$, Bi_2O_3, Fe_2O_3, Nb_2O_5, $CaZr_2O_3$, Er_2O_3, Yb_2O_3, Ho_2O_3), concentration from 0.01wt% to 1wt%, consolidated under the pressing pressure up to 150 MPa and 1180°C-1380°C sintering temperatures, are used. We performed SEM and EDS analysis.

The fractal nature offers a new approach for the ceramics structure analysis, describing, prognosis and modeling the grains shape and relations between ceramics structure and electric-dielectric properties. The microstructure has a great importance from different alternative energies points of view. World's interest race in renewable and new generation energy sources development, especially the new batteries systems, are in research and development focus, simultaneously, in the electric cars technologies development. Beside the electrochemical processes and rechargeable speed, the storage capacity has special significance which is enriched by the fractal natureanalysis and these scientific paper contributions with some fundamental electrochemical laws through fractal corrections expressed by the relevant formulas. These are the new frontiers in direction of electrochemical fractal microelectronics. Also, the wind energy as new and alternative energy source has important role growing.

The land and obstacles of fractal nature, influence on air/wind turbulence towards the wind generators propellers, has special effect on the wind speed, described by the logarithmic law equation which is deduced from the similarity theory that is strictly applicable to steady-state horizontally homogeneous conditions in the surface layer. So, definitely in this paper the fractal nature independently existing everywhere within the structures, contact surfaces, practically, from microstructures, even on nano level up to global bulk and massive shapes, fractal nature ceramics materials existence is completely confirmed within the electrochemical thermodynamic and fluid dynamics parameters, are confirmed.

Keywords: *alternative energy, $BaTiO_3$-ceramics, Coble's model, microstructure, fractals, electrochemical energy, wind generators.*

INTRODUCTION

Fractal nature analytic method in materials structure reconstruction, grains and pores, in order to make an advance designed microstructure properties prognosis, is a new procedure in materials microstructure characterization [1-4]. Electronic microscopy methods, regardless on resolution and magnification, enables getting the micrographs. This was applied on barium-titanate, silicate, refractory and other ceramics, but can be applied also to any material. Based on the grains and perimeters fractal analysis, their reconstruction is made by using Richardson method of variable yardstick (Figure 1). It gives a more realistic picture as is obtained by the Euclidean geometry frame, which replaces the role of modeling, because it gives real micrographs shapes, on one hand, and from the obtained passive micrograph, through the shape reconstruction, leads to its prognoses possibility with designed microstructure properties [5]. Applying the known technology process syntheses phases, obtained samples are the investigated objects, leading toward a more ceramics electronic materials properties exact calculations.

The characterization materials data, by SEM, does not have opportunity to play the active role with, once reconstructed microstructure shapes in the function to the microstructure properties prognosis. All available microstructure analyses tools are only a passive instrument to get characterization data, so the fractal nature structure analysis practically making all of these known methods more alive and applicable for developing future needs, especially in the microelectronics miniaturization area [6].

From this point of view, all the most modern and maximal optimized microstructure methods are faced, with open question, how to provide more flexibility on the field of the structure units (grains and pores) reconstruction and their interrelations with the final goal to be in function of a future higher levels, better packaging, microelectronic components and devices and electronic integrated circuits, integrations. So, the new frontiers opening, based on materials structure fractal nature, was practically very important natural necessity in the triad contact point: much deeper material characterization – the structure constituents (grains and pores) reconstruction – predicting the microstructure properties within the miniaturization frame [7].

The “fractal nature structure analysis – fractal electronics” relation, is practically the new scientific approach, immediately after nanoscience and technologies.

The intergranular contacts inside the perovskites and other electronic ceramics materials, generally in all ceramics, we understand, nowadays, as the intergranular capacities real structure nature, and use that as a capacities phenomenon explanation (Figure 2). These fractal nature phenomena are stressed in a set of papers, in the form of a correction factor α that we added as a multiplicative constant for the ceramics material relative permittivity ε_r; instead of ε_r in all formulas we set $\alpha\varepsilon_r$, with a hypothesis that the real number α compensates increasing capacity which comes from the intergranular contacts. One approach is to estimate the α value to lead it out from the outline fractal dimension or the ceramics grains and pores surface fractal dimension. In the meantime, this was more developed as one very exciting idea.

In that sense, we will take in consideration some of equations, as the Gibbs free energy equation, the Gibbs free energy (ΔG), the cell potential ($E°cell$) and the equilibrium constants (K) connection equation and the Butler-Volmer equation.

The new energy and alternative sources become the most perspective area in research and application. The clean and renewable wind energy, is one of the most promising. A little change of the wind and air fluid parameters might influence instability in wind energy systems. The wind speed and other fluid dynamic parameters are very important for wind energy systems performances. The fractal nature parameters characteristics were analyzed. Nowadays, the chaos theory concept is gradually adopted in many applications, also in wind field by fractal analysis. The fractal characteristics of the wind speed and other parameters are studied. The fractal analysis in the wind speed area are very rare in the world’

scientific relations. The first results within the Mitić-Kocić fractal approach have been done as intergranular fractal capacitor.

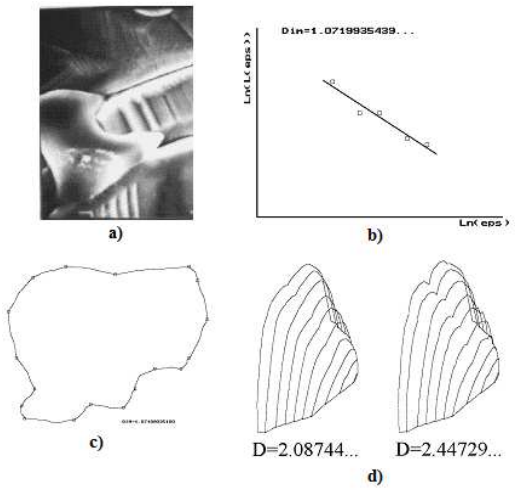

Figure 1. a) $BaTiO_3$ SEM micrograph, b) fractal diagram, c) $BaTiO_3$ grain' contour shape, d) grain surface model of different fractal dimensions

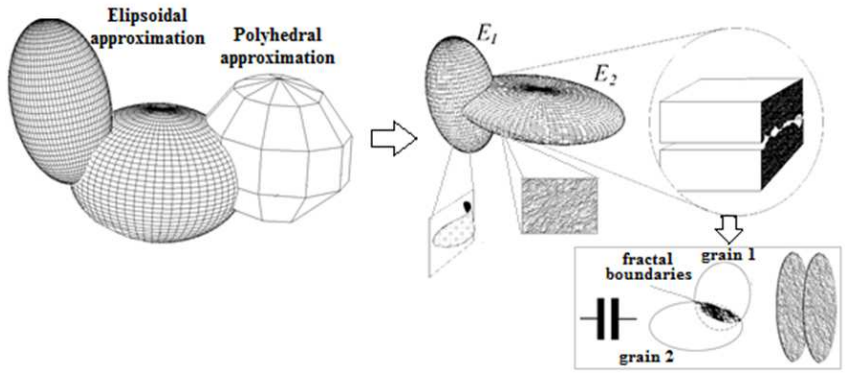

Figure 2. Euclidean geometry to fractal intergranular capacitors

Figure 3 shows the relationship between the surface area *A*, its fractal dimension *D* and the stride *δ*.

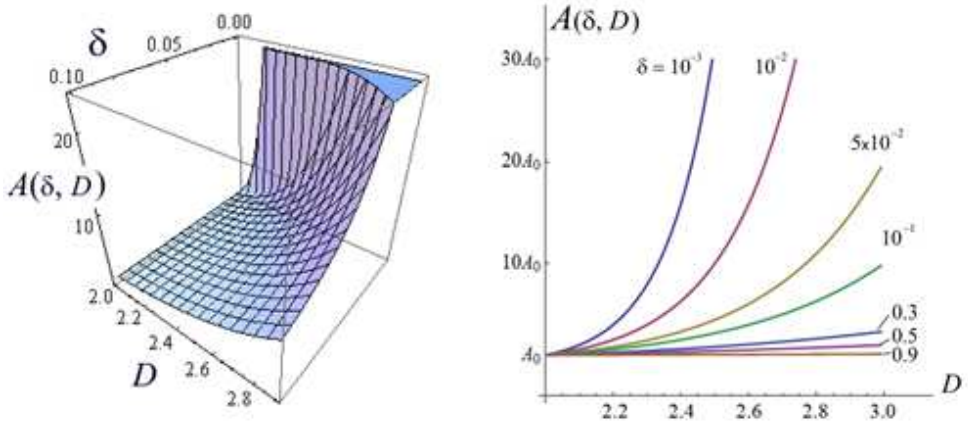

Figure 3. a) Size of the contact area A(δ, D)vs. fractal dimension DH_f;
b) Increasing of the area size depends on fractal dimension and measurement unitδ

Such considerations helped us to estimate the capacity of one micro-contact that occurs between two neighbor ceramics grains:

$$C = \alpha \varepsilon_0 \varepsilon_r \frac{A(DH_f)}{d} \tag{1}$$

so

$$C = \alpha \varepsilon_0 \varepsilon_r \frac{Const \times \delta^{2/D-2}}{d} = K\delta^{2/DH_f - 2} \tag{2}$$

where δ is yardstick (stride), A area of the contact surface. From the last two formulas it is clear that the surface area increases when δ gets smaller; theoretically, for $1<DH_f$, $A \to +\infty$ when $\delta \to 0_+$.

EXPERIMENT

In this paper, it was necessary to prepare a samples series based on $BaTiO_3$-ceramics, for further investigations related to the microstructural and electrical characteristics interdependence optimization and for concrete fractals applications involvement. The pressing pressure, sintering conditions (temperature, sintering time), and the additives content on the microstructure influence and thus on the final $BaTiO_3$-ceramics characteristics, have been investigated.

For the research, pure $BaTiO_3$, as well as a powder based on $BaTiO_3$, with the additives (CeO_2, $MnCO_3$, Bi_2O_3, Fe_2O_3, $CaZr_2O_3$, Nb_2O_5, Er_2O_3, Yb_2O_3, Ho_2O_3, La, Sm, Dy) from 0.01wt% to 1wt%, were used. Complete experimental procedure is shown in Figure 4 [8].

After measuring a pure $BaTiO_3$ and additives powders, the mixture was processed into a mill with balls, in which a certain water and an organic binder amount, was added. Homogenization was carried out for about 48 hours. Mass was transported to the sprayer by membrane pump, where it was dried; thus determined powder granulation was obtained. Then, the material was collected in a special vessel, and its bulk density was investigated every hour. Occasionally, a granulation analysis was performed by vibrating sieve, which was essential for pressing. The powder particles were spherical shape (size 10-130 µm), with the particles agglomerates appearance. The presented powders process preparing is fully applied in a pure $BaTiO_3$ powder consolidation.

In order to investigate the pressing pressure influence, i.e. the green density preforms influence on the obtained samples characteristics, a pure $BaTiO_3$ samples double-sided pressing with pressures from 35 to 150 MPa and different $BaTiO_3$-ceramics based on mixture with additives powders green density, were formed. The samples pressing was done on a hydraulic press (JAPAN KYOTO Murata B1) by using a tool which is also applied for multi-layer capacitor technology, the sample square shape forming.

Sintering was performed in an electric tunnel furnace (CT-10 Murata) at temperatures from 1180°C to 1380°C (Figure 4.c). The samples are located in special containers (saggers), during the 38 sintering hours. For easy separation after sintering, the samples are covered with refractory special powder-sand before sintering.

Based on such consolidation, the different sintering temperature (from 1320°C to 1380°C), as well as different additive concentration, for example Ho_2O_3 (from 0.01wt% to 1wt%) influence on the $BaTiO_3$-ceramic grain density and size were investigated. For Ho_2O_3 doped $BaTiO_3$, density varies from 80% of theoretical density (TD) for high doped samples (1wt% of Ho_2O_3) sintered at 1320ºC, to 93% TD for low doped samples (0.01wt% of Ho_2O_3) sintered at 1380ºC. By dopant concentration increase, the grain size decreases. As a result, for 0.5wt% of dopant the average grain size was from 10 µm to 15 µm, and for the samples doped with 1wt% of dopant grain size decreased to the 2-5 µm for both sintering temperatures.

The new possibilities, in microstructure characterization applications, are directly introduced, with which the hardware is reduced only to presented engineering system, providing new solutions related to software support. Such solution opens industrial production and application possibilities, and that is a base for the Fractal electronics development.

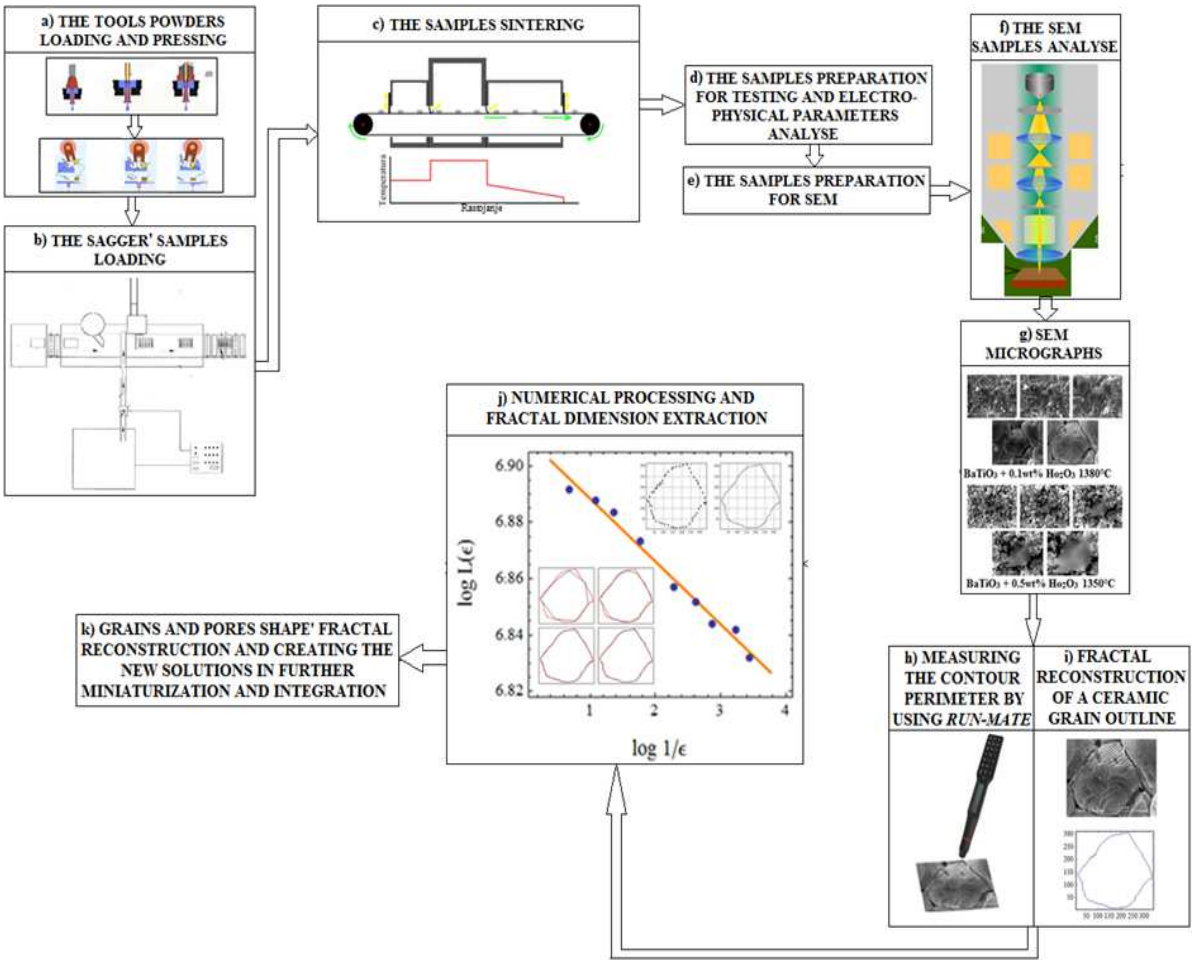

Figure 4. Experimental procedure

Thus prepared samples were analyzed by SEM (JEOL JSM-5300) equipped with EDS (QX2000S) for additives concentration investigations (Figure 4.f). The microstructure analysis was performed under different magnifications (from x750 to x35,000).SEM images of Ho_2O_3 doped $BaTiO_3$ are shown in Figure 5.

In the early research and development stages, a small measuring device *Run-mate* (Figure 4.h), which measures the contour perimeter in a given image plane, is applied in order to apply the box-counting method to retrieve the *fractal dimension*, DH_f, which is the most important quantity involved with the notion of fractals being introduced by Mandelbrot. The fractal dimension, which is a natural extension of the usual notion of dimension which is usually called *topological* (or *geometric*) *dimension*. The obtained perimeter data, for at least five different magnification of the same observed grain, presents the basis for data obtaining that can be applied to the Richardson' law and to further grain shape fractal reconstruction procedure.

Each of these micrographs, which are obtained with the SEM microscope in digitized form, typically in a 1808x1440 resolution in an 8-bit gray scale, could be further processed in some graphical editor (Figure 4.i). The selected ceramic grain's contour transfers into analytic form applying fractal interpolation procedure introduced by Barnsley. After perimeter points samples acquisition, the fractal

interpolation is applied. The result is a set of piecewise linear parametric functions defined by an iterative procedure.

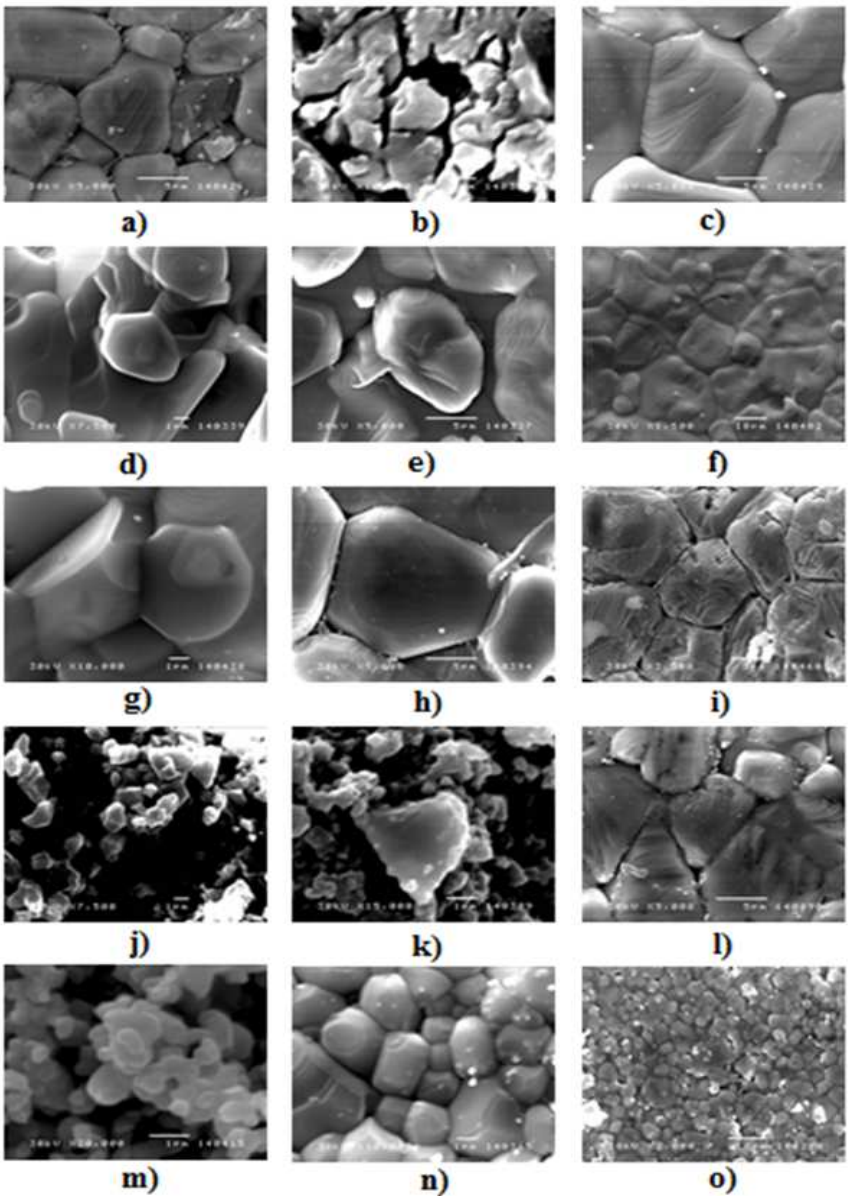

Figure 5. SEM images of Ho_2O_3 doped $BaTiO_3$
a) 0.01wt%, 1320ºC, b) 0.01wt%, 1350ºC, c) 0.01wt%, 1380ºC,d) 0.05wt%, 1320ºC, e) 0.05wt%, 1350ºC, f) 0.05wt%, 1380ºC, g) 0.1wt%, 1320ºC, h) 0.1wt%, 1350ºC, i) 0.1wt%, 1380ºC, j) 0.5wt%, 1320ºC, k) 0.5wt%, 1350ºC, l) 0.5wt%, 1380ºC, m) 1wt%, 1320ºC, n) 1wt%, 1350ºC, o) 1wt%, 1380ºC

In the early research and development stages, a small measuring device *Run-mate* (Figure 4.h), which measures the contour perimeter in a given image plane, is applied in order to apply the box-counting method to retrieve the *fractal dimension*, DH_f, which is the most important quantity involved with the notion of fractals being introduced by Mandelbrot. The fractal dimension, which is a natural extension of the usual notion of dimension which is usually called *topological* (or *geometric*) *dimension*. The obtained perimeter data, for at least five different magnification of the same observed grain, presents the basis for data obtaining that can be applied to the Richardson' law and to further grain shape fractal reconstruction procedure.

Each of these micrographs, which are obtained with the SEM microscope in digitized form, typically in a 1808x1440 resolution in an 8-bit gray scale, could be further processed in some graphical editor (Figure 4.i). The selected ceramic grain's contour transfers into analytic form applying fractal interpolation procedure introduced by Barnsley. After perimeter points samples acquisition, the fractal

interpolation is applied. The result is a set of piecewise linear parametric functions defined by an iterative procedure.

It should be mentioned that all these steps, which have the microstructure analysis experimental character by microscope, as well as grain perimeter data collection, are, in fact, part of a completely new ceramic materials, and materials in general, grain and pore structure microstructural characterization methods. This is a characterization methods innovation, which allows the microscopy different types applications.

RESULTS AND DISCUSSION

The experimental-theoretically data collection procedures for fractal analysis have appropriate mathematical support for the grains and pores shape fractal reconstruction [9].

The acquisition of perimeter sample points are read in the form $(x_i, y_i)_1^n$, which are points selected according to the representative expression criteria, and the result is the manipulators assessment. The total number of points, n, depends on the contour complexity and it typically ranges from 40 to 70. By applying the Barnsley' algorithm, fractal interpolant for the x and y particular component are obtained (the functions f_x and f_y), so the contour is reconstructed in the parameter form (f_x, f_y), then again in the points series form, their number is now increased to $n(n + 1)$, because, between every two points, a new $n + 1$ points, are inserted. Thereby, obtained the real contours polygonal approximation in $n + 1$ higher resolution than the contour which is represented by the starting point (Figure 4.j).

On the other hand, to understand this complex solutions, separately how the fractal dimension, which is very important in microstructure fractalization, is calculated by using the Richardson' law, is explained. In this sense, the Richardson' law application can be explained by using the asymptotic power-law formula:

$$L(\delta) \sim K\delta^{1-DH_f} \tag{3}$$

where δ is the polygon side length inscribed in the grain contour, and $L(\delta)$ is the polygon perimeter, DH_f is the contours fractal dimension and K is a positive constant. This formula is asymptotic, which means, and it is more accurate as soon as the polygon side length δ is closer to zero. In this case, when the δ approaches to zero, the asymptotic equality sign (~), may be replaced with the equality sign, which gives:

$$\log L(\delta) = \log K + (1 - D)\log \delta \tag{4}$$

or

$$D - 1 = -\frac{\log L(\delta)}{\log \delta} + \frac{\log K}{\log \delta} \tag{5}$$

and since the K is a constant,

$$\lim_{\delta \to 0} \frac{\log K}{\log \delta} = 0 \tag{6}$$

one makes,

$$D - 1 = \lim_{\delta \to 0+} \frac{\log L(\delta)}{\log 1/\delta} + \frac{\log K}{\log \delta} \tag{7}$$

The right side limes can be approximately determined from the $y = \alpha x + \beta$ slope in the x, y-coordinate system, that best approximates a points set ($x_i = \log 1/\delta_i$, $y_i = \log L(\delta_i)$) in the least-square metric. The δ_i, $i = 1, 2, ..., m$, are the side lengths of the inscribed polygon, and $L(\delta_i)$ is the appropriate perimeter in the i^{th} iteration. In each m iteration, the polygon sides lengths do not have to be equal, and in this case, δ_i is the maximum side length in the i^{th} iteration (Figure 4.j).

The line slope α is the only quantity that is required, and the least-square approximation formula gives:

$$\alpha = \frac{\sum \log(1/\delta_i) \sum \log L(\delta_i) - m \sum \log(1/\delta_i) \log L(\delta_i)}{\left(\sum \log(1/\delta_i)\right)^2 - m \sum \log^2(1/\delta_i)} \tag{8}$$

From (7), it follows $D = 1 + \alpha$, and thereby, the contour fractal dimension approximate value, which is required, is obtained.

In order to increase the procedure applicability, the use of microstructural analysis and results in further electronic miniaturization and integration development, within the Fractal electronics, is anticipated.

The applied method application gives the possibility of faithful grains and pores shapes reconstruction as ceramic materials microstructural constituents, and materials in general, on the one hand, and on the other hand, all the reconstructed elements can be used in prognosis and designing important pre-defined microstructure properties.

The fractal dimension DH_f of a typical grain's surface is just slightly above surface's topological dimension, $D_T = 2$, and the difference $DH_f - D_T = DH_f - 2$, is thereby supposed to be responsible for ferroelectric phenomena affection; that cannot be explain by purely grain surfaces Euclidean geometry. Because the measured fractal dimension differs throughout the ceramics material, it is suitable to introduce a *normalized surface fractality parameter* α_S

$$\alpha_S = \frac{1}{\max\{DH_f\} - \min\{DH_f\}} \left(DH_f - \min\{DH_f\}\right) \tag{9}$$

which ensures the unit range $0 < \alpha_S < 1$.

But, most of perovskites and other electronic-ceramics materials are also porous materials, that correspond to a lacunar fractal models, as a new phenomenon; solidification of porous and "spongy" materials increases overall fractal dimension from (theoretically) 2 to full solid 3 ($2 < DH_P < 3$). It generates another correction factor, "α-pores",

$$\alpha_P = D_T - DH_P \tag{10}$$

where D_T is dimension of the space and DH_P is corresponding fractal dimension of a porous configuration. Therefore, $0 < \alpha_P < 1$. By their geometric root, the dimensionless quantities α_S and α_P will be called *geometric fractality factors*.

As the next, we are aware of the existence of the third (dimensionless) factor α_M carrying over the influence of disorder movement of ferroelectric particles that is factor of fractal movements.

There is a moving particles "cloud" in semiconductors (and metals as well) consists of electrons in atoms with large atomic numbers, nucleons in heavy atomic nuclei, and gases consisting of quasi particles with half-integral spin. This is called Fermi gas and obeys Fermi-Dirac statistics which are useful for further ideas development in this area.

Fractals and Electrochemistry Energy Area Application

Real Fermi gas dynamics impose necessity of fractal movements factor α_M inclusion, that makes third factor, next to geometric ones α_S and α_P. Since Fermi gas particles have dynamics similar to 3D Brownian one, α_M should be derivate of Hausdorff fractal dimension DH_M of a Brownian 3D space-filling curve. It is obvious that $1 \leq DH_M \leq 3$. The lower limit, $\min D_M = 1$, is imposed by a particle trajectory continuity. The upper limit, $\max D_M = 3$, in turn is the maximum of trajectory complexity in 3D space. It is reasonable to normalize quantity α_M, by taking.

$$\alpha_M = \frac{1}{\max\{DH_M\} - \min\{DH_M\}} \left(DH_M - \min\{DH_M\} \right) \tag{11}$$

which ensures $0 < \alpha_M < 1$.

By this way, three independent dimensionless fractality factors α_S, α_P and α_M are introduced. These are real numbers from the open interval (0, 1) [10, 11].

Our hypothesis is that electronic-ceramics working temperature must be influenced by these three fractality factors, making correction of „theoretic" temperature T, to get the new "real" temperature T_r, which is temperature actually lower than T which is affected by the material inner fractality, and thereby $T_r = T - \Delta T$. Obviously, $T_r \leq T$ with equality if no fractal structure of *S*, *P* or *M* type is present; by setting

$$\alpha = \frac{T_r}{T} = 1 - \frac{\Delta T}{T} \tag{12}$$

one has $T_r = \alpha T$ where, α is depends on all three alpha-components α_S, α_P and α_M given by (9), (10) and (11), so,

$$\alpha = \Phi\left(\alpha_s, \alpha_P, \alpha_M\right) \tag{13}$$

For example, by the Curie-Weiss law [12], the relative permittivity will be given by

$$\varepsilon_r = \frac{C_c}{T_r - T_C} = \frac{C_c}{\alpha T - T_C} = \frac{C_c}{\Phi\left(\alpha_s, \alpha_P, \alpha_M\right) T - T_C} \tag{14}$$

where $C_c = 1.7 \text{x} 10^6$ K is the Curie constant what is the natural way to demonstrate the ceramics fractal nature influence on dielectric constant. The capacity is slightly higher than it will be if the ceramics fractal nature is neglected.

We underline that the function Φ is unknown up to now, but a good approximation would be a linear combination of α_S, α_P and α_M,

$$\alpha = \Phi\left(\alpha_s, \alpha_P, \alpha_M\right) = \omega_1 \alpha_S + \omega_2 \alpha_P + \omega_3 \alpha_M, \tag{15}$$

where $\omega_1, \omega_2, \omega_3 \geq 0, \ \omega_1 + \omega_2 + \omega_3 = 1$, are so called *barycentric coefficients*. The identity (15) ensures boundedness of the function Φ (and so of α as well), i.e.,

$$\min(\alpha_S, \alpha_P, \alpha_M) \leq \Phi\left(\alpha_s, \alpha_P, \alpha_M\right) \leq \max(\alpha_S, \alpha_P, \alpha_M) \tag{16}$$

Regarding the previous Fractal microelectronics frontiers and after the fractal correction, Gibbs free energy, the Gibbs free energy, the cell potential and the equilibrium constants connection and the Butler-Volmer dependence of the temperature equations, will have the following form:

Gibbs free energy equation:

$$G\left(p, T\right) = U + pV - T_r S \tag{17}$$

or

$$G(p,T) = H - T_r S \tag{18}$$

where U is the internal energy, ρ pressure, V volume, S the entropy and H the enthalpy.

ΔG, E°cell and K connection equation:

$$\Delta G^\circ = -RT_r \ln K = -nFE^\circ_{cell} \tag{19}$$

where $R$is universal gas constant, n moles of e^- from balanced redox reaction and F the Faraday's constant.

Butler-Volmer equation:

$$I = A \cdot j_0 \cdot \left\{ \exp\left[\frac{a_a nF}{RT_r}\left(E - E_{eq}\right)\right] - \exp\left[-\frac{a_c nF}{RT_r}\left(E - E_{eq}\right)\right]\right\} \tag{20}$$

or

$$j = j_0 \cdot \left\{ \exp\left[\frac{a_a nF\eta}{RT_r}\right] - \exp\left[-\frac{a_c nF\eta}{RT_r}\right]\right\} \tag{21}$$

where I is electrode current, Aelectrode active surface area, j electrode current density, j_0 exchange current density, E electrode potential, E_{eq} equilibrium potential, n number of electrons involved in the electrode reaction, $\alpha_c$so-called cathodic charge transfer coefficient, α_a so-called anodic charge transfer coefficient, η activation overpotential.

Simultaneously, by these fractal corrections within the electrochemical equations thermodynamic parameters, it is very important to demonstrate our fractal research performances as very powerful "tool" for reconstruction of the microstructure constituents, like grains and pores are.

Once having the fractal dimension, this "tool" may offer a pretty well reconstruction of the contour of a ceramics grain, using fractal interpolation procedure and characteristic sample data.

The studying base is a set of micrographs, obtained with the SEM microscope, by *Run-meter* grain' perimeter measurement or in digitized form, typically in a 1808x1440 resolution in an 8-bit gray scale, is further processed in some graphical editor. The selected ceramic grain's contour transfers into analytic form applying fractal interpolation procedure introduced by Barnsley (Figure 6). After perimeter points samples acquisition, the fractal interpolation is applied. The result is a set of piecewise linear parametric functions defined by an iterative procedure.

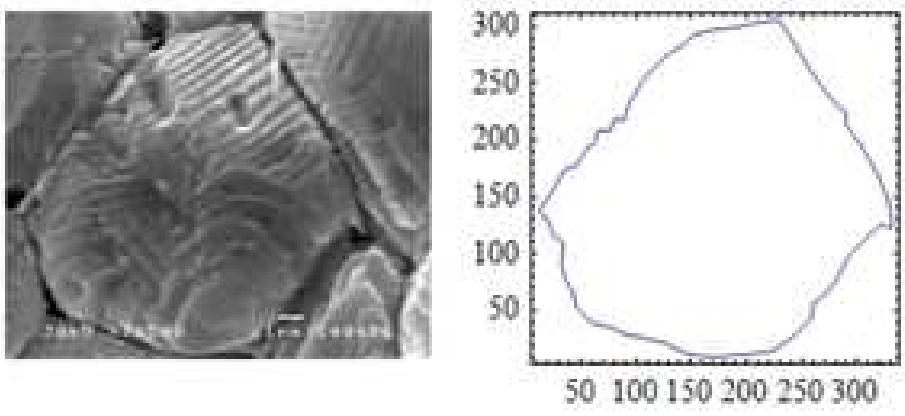

Figure 6. Fractal reconstruction of $BaTiO_3$-ceramics grain outline.
1μm on the SEM corresponds to 20 units in the reconstruction right

Fractals and Wind Energy Applications

Based on development research, we can present the fractal correction parameters influence on air/wind dynamic new results[13]. As it is well known from the air fluid dynamic, general equations are:

$$\frac{du}{dt} = -\frac{1}{\rho}\frac{\partial p}{\partial x} + lv$$
$$\frac{dv}{dt} = -\frac{1}{\rho}\frac{\partial p}{\partial y} - lu$$
$$\frac{dw}{dt} = -\frac{1}{\rho}\frac{\partial p}{\partial z} - g \tag{22}$$

where $\frac{du}{dt}, \frac{dv}{dt}, \frac{dw}{dt}$ are components of air acceleration. After transformations, which are including molecular or turbulent viscosity, the continuity equality, the equality of state and the adiabatic equality, we have:

$$\frac{dT}{dt} = \frac{c_p - c_v}{c_p}\frac{T}{p}\frac{dp}{dt} + \frac{1}{c_p}\frac{T}{p}\frac{dQ}{dt} = \frac{\gamma a}{g\rho}\frac{dp}{dt} + \frac{1}{c_p}\frac{dQ}{dt} \tag{23}$$

In the lower atmospheric layers, tangential stresses τ'_{yx} and τ'_{zx} become dominant. In addition, the ground layer is characterized by constant values of τ'_{yx} and τ'_{zx} which means that wind direction does not change by height. The thickness *H* of this ground layer may range between 20m and 100m. It is anyway widespread accepted *H* = 50m.

Turbulence may be characterized by *L* – ratio of turbulence. Propose that the stress τ depends only on vertical velocity gradient, density and turbulence ratio:

$$\tau = \rho L^2 \left(\frac{\partial \bar{u}}{\partial z}\right)^2 \tag{24}$$

On the other hand, it is reasonable to take $L = kz$ where *k* is dimensionless (*Von*) *Karman's constant*, describing the logarithmic velocity profile of a turbulent fluid flow near a boundary with a *no-slip condition*.

By analogy with (24), the turbulent atmosphere η can be replaced by $k\rho$, so that:

$$\tau = k\rho \left(\frac{\partial \bar{u}}{\partial z}\right) \tag{25}$$

Comparison with (24) gives turbulence coefficient:

$$k = u_0 L = u_0 kz \tag{26}$$

where the friction velocity u_0 represents *shear stress* term τ_ω for the fluid of density ρ, and *k* is Karman's constant. Now, from (24) and (26), one deduces the wind profile differential equation

combines the *mean horizontal wind velocity* $\bar{u}$ blowing on the height *z* above the surface, under near-neutral conditions and with a homogeneous distribution of obstacles,

$$\frac{\partial \bar{u}}{\partial z} = \frac{u_0}{kz} \tag{27}$$

After integration, where z_0 is known as *roughness length* (or *roughness height*), which is the height (above the surface) where the wind has zero speed, we have the *wind profile logarithmic law*:

$$\bar{u}(z) = \frac{u_0}{k} \ln \frac{z}{z_0} \tag{28}$$

It is empirically set that

$$\frac{1}{10} h \le z_0 \le \frac{1}{30} h \tag{29}$$

where *h* is the height of the obstacle to the wind. So, using wind profile logarithmic law (28), the wind speed v_r, on the referent height z_r, and *v* some other height *z*, one gets

$$v_r = \frac{u_0}{k} \ln \frac{z_r}{z_0}$$
$$v = \frac{u_0}{k} \ln \frac{z}{z_0} \tag{30}$$

where from follows

$$\frac{v}{v_r} = \frac{\ln(z/z_0)}{\ln(z_r/z_0)} = \frac{\ln z - \ln z_0}{\ln z_r - \ln z_0} \tag{31}$$

The logarithmic law (28) can be derived from the Monin-Obukhov [14] similarity theory that is strictly applicable to steady-state horizontally homogeneous conditions in the surface layer. This theory says that statistical characteristics in flow dynamics are invariant with respect to similarity transformation $[x\ y]^T \to [ax\ ay]^T\ (a>0)$ and it is valid for $z \gg z_0$. In praxis, the limits (29) for z_0 are used, with the constants λ_1= 1/10 to λ_2 = 1/30. But, in more accurate setting, both λ_1 and λ_2 may vary depending on the environmental parameters, so it will be reasonable to use linear interpolation

$$z_0 = (1-\theta)\lambda_1 h + \theta \lambda_2 h,\ 0 \le \theta \le 1 \tag{32}$$

If we take into account fractality of the obstacles, the different formulas can be approached. Indeed, if an obstacle is some forest then, an intuitive image of some contains "thickness" as a first parameter. Some forests, lake these in polar areas are very sparse. On the other hand, some tropical forests are impossible to pass through. Some canopies are made of tinny leafs some has large heavy leaves, so that they absorb larger amount of energy from the wind blowing through such forest. The same is with crops, habitats, rocks, mountains etc.

The "thickness" of the obstacle can be measured with fractal (Hausdorff) dimension H_d. The object of the average height *h*, can have fractal dimension between 2 and 3. In fact H_d = 2, for an ideally flat ground surface. The other extreme, H_d = 3 is reserved for a solid wall or hill cliff with enough horizontal dimension in direction orthogonal to the wind vector, to prevent the wind passing. In this case, we may set $\lambda_2 \to +\infty$, which implies nonlinear formula that will replace (32), and it is

$$z_0 = \frac{\lambda_1 h}{3 - H_d},\ 2 \le H_d \le 3 \tag{33}$$

For ideally flat ground, $H_d = 2$, so that (33) yields $Z_0 = \lambda_1 h$. From the dense point of view, impenetrable obstacle, $H_d = 3$, which gives

$$z_0 = \lim_{H_d \to 3} \frac{\lambda_1 h}{3 - H_d} = +\infty \tag{34}$$

which is equivalent as $\lambda_2 \to +\infty$.

After all, the wind profile logarithmic formula (28) becomes

$$\bar{u}(z) = \frac{u_0}{k} \ln \frac{z}{\lambda_1 h}(3 - H_d) \tag{35}$$

while (31) gives

$$v = v_r \frac{\ln z + \ln(3 - H_d) - \ln(\lambda_1 h)}{\ln z_r + \ln(3 - H_d) - \ln(\lambda_1 h)} \tag{36}$$

The mean horizontal wind velocity depends on the logarithm of the constant z_0 (in meters) known as the *roughness height* since it depends on the roughness surface over which the wind blows. Here, we suggest a refinement of the "classic" z_0 estimation by the mowing average formula controlled by the unitary interval parameter θ, which is recognized as a linearization of the more natural form containing fractal dimension of the surface H_d, which replaces the linear law by a hyperbolic one.

So, finally, the first time in air fluid science, we have fractal correction based on different land obstacles influence involved in wind velocity equations which directly influence on wind generator propeller motions.

From the fractal nature point of view, the microstructure roughness on the grains and pores surfaces, have the same position like the global phenomenological land shapes. So, the mountains, hills and vales on the Earth, observed by the space telescope are mostly similar to sub-micro roughness and shapes on grains and pores surfaces.

CONCLUSION

This paper has significance from the ceramics microstructure consolidation prognosis fractal aspect point of view and possibility of having better insight into some internal properties such as intergranular microcapacity. There is existing influence of ceramics grains' surface fractality plus particle dynamics in the material on the overall energy distribution. It is pretty efficient since the upper error limit in grains shape reconstruction rarely exceeds 3%. Such experimental-theoretical model clarifies the relationship between energy and fractality what is the key factor in final material property prognosis. High precision of the applied fractal nature mathematics opens the new perspectives to better intergranular capacity evaluation and micro-impedances spatial distribution understanding with the further miniaturization and electronic circuits integration frontiers. With this, we can proceed towards better components and devices packing because the semiconductor technology possibilities are already limited.Presented experimental-research and theoretical work is the extended investigations part in the materials structures analysis area, and the fractal nature domain, which is important for more precise contact surface in energy storage area and in materials consolidation for battery systems. These results confirm microstructure constituent's shapes, grains, reconstruction possibilities with Brownian motion particles application, by long term scientific research on the

electronic materials fractal analysis. This is original contribution in the basic electrochemical thermodynamic parameters area by introducing the α, fractal correction function, having as the arguments three correction parameters α_S, α_P and α_M, as electrochemistry area functions, especially from the energy storage aspects and creating new approach towards intergranular capacity. This offers a solid base for the future procedure and further application, to create new perspectives and solutions for advanced miniaturization, electronic parameters multi-level integration, materials, components and circuits (especially *C*, *R*, *L*) characteristics, as well as new solutions for better components and electronic circuits packaging (Figure 4.k).

All of these is of huge importance for the new and alternative energy sources, as the new frontiers towards miniaturization, what is in the new experimental-theoretical approach frame in the new [8] model line, which could consider as the electrochemistry area Fractal microelectronics. From the other side, this paper is a systematic approach to create the method for the wind motion and turbulences, prognosing the fractal nature influence. One of the most important thing is the wind parameters fractal analysis for different terrain roughness profiles. Definitely, this is the first time in air fluid science that we have recognized the fractal nature influence within the matter. In this way, we confirmed the new fractal frontiers in the area of alternative energy sources, what is very new, precise and powerful approach. The concept design main goal is to reach the inventive ideas for final products with best performances.

Through this method and results, we are opening the Fractal microelectronic new frontiers and technological processes, especially specific intergranular relations within grains surfaces coatings. This enlightening the new future intergranular thin film's fractal nature microelectronics, from the one aspect, and also opening the new "window" towards that the sizes of the objects on the Earth, under the telescope from the space, are like microstructures under the microscope, from the other aspect regarding the fractal nature in the matter.

From that aspect the relation large-small in the light of fractal analysis is very important. An ideal fractal can be magnified endlessly but natural morphologies cannot. This is the reason why natural objects cannot be ideal fractals. The exception is maybe the Universe as whole. Our microstructures do not differ regarding fractality from macrostructures. The practical question is what is the measure range in which fractality can be identified? By rule, the minimum information we need must be ranged in at least 3 orders of magnitude. For example, on the level of 1 micron, 10 microns and 100 microns, although it gives a very rough estimation. More acceptable model understands 6 to 7 orders of magnitudes. Since our typical grains are 50 microns large, in average, we need magnification that reveals more or less 50 grains which supposed the "window" of about 3000 microns in diameter. The next will be 300 microns, then 30 microns (focusing one grain), 3 microns, 300 nm and finally 30 nm.

This will be enough for fractal dimension DH_f to be estimated with error of 3 to 5%. The error can be reduced down to 1% by combining successive magnification with some geometric actions, for example by SEM picture rotations for some angle and by procedure repeating. The other way is to analyze several details, at the same time. Anyway, fractal dimension accuracy increasing needs good choice of the scaling range. For example, if one needs to determine $DH_f$for an oak leaf, it is pointless to begin an oak observation from the distance of 5 km, since the oak canopy looks as a point, which results as zero starting dimension.Also, leaf surface magnification to the nanometer level will not reveal any information about a leaf as a whole but the picture of molecular structure of starch in leaf cells.

ACKNOWLEDGEMENT

This research is a part of the project „Directed synthesis, structure and properties of multifunctional materials" (172057). The authors gratefully acknowledge the financial support of Serbian Ministry of Education, Science and Technological Development for this work.

(Received December 2015, accepted December 2015)

REFERENCES

[1] Mandelbrot, B. (1983). The Fractal Geometry of Nature, W. H. Freeman and Co., New York.
[2] Barnsley, M. (1988). Fractals everywhere, Academic Press.
[3] Mandelbrot, B. (1975). Les objets fractals, forme, hasard et dimension, Flammarion, Paris.
[4] Mitić, V.V. (2001). Structure and electrical properties of $BaTiO_3$-ceramics, Monography, Andrejević Foundation, Belgrade, Serbia.
[5] Mitić, V. V., Kocić,Lj. M., Mitrović, I., Ristić, M. M. (1997). Models of $BaTiO_3$ Ceramics Grains Contact Surfaces, The 4th IUMRS International Conference in Asia OVTA Makuhari, Chiba, Japan.
[6] Mitić, V. V., Pavlović, V. B., Kocić,Lj. M., Paunović, V., Mančić, D. (2009). Application of the Intergranular Impedance Model in Correlating Microstructure and Electrical Properties of Doped $BaTiO_3$, Science of Sintering, Vol. 41, No. 3, pp. 247-256.
[7] Mitić, V.V., Paunović, V.,Kocić,Lj. (2015). Fractal approach to $BaTiO_3$-ceramics micro-impedances, Ceramics Int. 41 (5),pp. 6566–6574.
[8] Mitić, V.V., Kocić,Lj. (2015). Fractal nature structure, grains and pores, reconstruction analysis method and application in advance designed microstructure properties prognosis function, Patent, Application number 2015/0152, Intellectual Property Office, Serbia.
[9] Thompson, H., Katz, A. J., Krohn, C. E. (1986). Method and means for determining physical properties form measurements of microstructure in porous media, United States Patent, Patent number (4,628,468).
[10] Bastić, F. (2014). The Fractal Nature Materials Microstructure Influence on the Battery Systems and Fuel Cells Energy Efficiency and Capacity Increasing, Ms Thesis, Faculty of Electronic Engineering, University of Niš, Serbia.
[11] Mitić, V. V., Kocić,Lj. M., Paunović, V., Bastić, F., Sirmić, D. (2015). The Fractal Nature Materials Microstructure Influence on Electrochemical Energy Sources, Science of Sintering, Vol. 47, No. 2, pp. 195-204.
[12] Mitić, V. V.,Paunović, V.,Kocić,Lj. (2014). Dielectric Properties of $BaTiO_3$ Ceramics and Curie-Weiss and Modified Curie-Weiss Affected by Fractal Morphology, in: Advanced Processing and Manyfacturing Technologies for Nanostructured and Multifunctional Materials (T. Ohji, M. Singh and S. Mathur eds.), Ceramic Engineering and Science Proceedings, Vol. 35 (6), pp. 123-133.
[13] Sirmić, D. (2014). Wind Energy as Alternative Source and Fractal Nature Analysis Application in Wind Generators Materials Consolidation, Ms Thesis, Faculty of Electronic Engineering, University of Niš, Serbia.
[14] Obuhov, A. M. (1988). Turbulentnost' idinamikaatmosfery, Gidrometeoizdat.